Struct Multidisc Optim (2017) 55:885–898
DOI 10.1007/s00158-016-1533-z

RESEARCH PAPER

Soap film analogy for anisotropically stretched membranes and cable nets

Valentina Beatini[1] · **Gianni Royer-Carfagni**[2,3]

Received: 15 September 2015 / Revised: 18 June 2016 / Accepted: 22 June 2016 / Published online: 22 July 2016

Abstract Analogical physical models are a preferred technique to intuitively grasp complex engineering problems. It is well-known that the equilibrium minimal-surface configuration of membranes under equibiaxial tension can be visually represented by the surface of a soap film under equivalent boundary conditions, but this analogy fails when the stress state is not uniform equibiaxial. We extend to this situation the analogy with soap films. The equilibrium state of an orthotropically tensioned membrane is found by geometrically stretching the shape of a soap film, in a precise manner depending upon the applied state of stress. The procedure is easily done by elaborating digital pictures. The method is mathematically justified under the kinematic hypotheses of small strains and large rotations, and further verified in a parametric design environment. It can also provide an insight into the equilibrium configuration of cable-nets, when the stresses in the warp and weft directions are considerably different. Furthermore, this visualization favors implementing transformable shapes for membranes or orthogonal cable nets, as a consequence of a modification of the ratio of the principal stress components.

✉ Valentina Beatini
valentina.beatini@agu.edu.tr

Gianni Royer-Carfagni
gianni.royer@unipr.it

[1] Department of Architecture, Abdullah Gul University, Kayseri, Turkey

[2] Department of Industrial Engineering, University of Parma, Parma, Italy

[3] Construction Technology Institute - Italian National Research Council (ITC-CNR), San Giuliano Milanese, Italy

Keywords Analogical model · Soap-film analogy · Minimal surface · Anisotropic tensioned membranes · Transformable architecture · Cable-nets

1 Introduction

This study illustrates a physical approach for defining the shape of membranes that are not under a uniform equibiaxial state of stress. Thence, this is not a design given once for all, but a design method which relies upon the natural properties of soap films. It is well-known, in fact, that soap films are optimal configurations for any assigned boundary: the state of stress is uniform equibiaxial and the deformation is that of minimal area. Here, a procedure to extend this analogical approach to the case of a non-equibiaxial stress state is provided. The method is quite intuitive and can be made immediately visible to designers. Furthermore, by analogy, the method can be extended to nets formed by orthogonal cables, when the load in the warp and weft direction is considerably diverse. Moreover, varying the ratio of the principal stress components (or equivalently the position of the boundary constraints), without producing slackening, represents a way to achieve a transformable architecture, i.e., a variation of the shape of the net to adapt to mutable environmental conditions or anthropic needs.

Following the proposed rationale, the designer can investigate optimal shapes through a form-finding algorithm, as opposite to a form-making approach. In the former, the final shape is found according to some optimality criterion whereas, in the latter, the shape is a target to be reproduced. Therefore, the method follows the architectural contemporary tendency to push from the path of appearance and representation *per se*, focusing instead on performances and processes. This process can be followed in the early stage of the design

phases as described in Guidon (1990), where emergent alternatives can help pursuing different solutions and imagining even more alternatives (Logan and Smithers 1993).

Such qualities are obtained thanks to a generative approach. With the term generative design, we refer to the broad definition given by Krish (2011), i.e., a design method composed of a design *schema*, a mean of creating variations and a mean of selecting desirable outcomes. In our case, there is a supporting analogy between variation in tension, in the membrane, and geometric distortion, in the soap film. Based upon this soap-film analogy, a set of qualitative considerations can be visually grasped by the designer, to be used as desiderata inputs for further tuning, up to achieving the desired result.

The basic idea is indeed quite classic, but to our knowledge it is the first time that it is extended to structures with a non-uniform equibiaxial state of stress. Soap films have been extensively used by Frei Otto to build surfaces working under tension only, such as membranes and cable nets (Nerdinger 2005). Similar intuitions were used in the same years by Heinz Isler and, before that, by Antoni Gaudí, who reproduced with their hanging cables and clothes, upside down, the optimal configuration of compressed vaults (Larena 2009). These architects intuitively designed form-active structures, i.e., structures defined by setting not the surface shape but the boundary conditions and the service load, opposite to form-made structures, where the shape is assigned. The analogic models were used for the consequent form finding processes, and they represented ingenious ways to overcome the lack of computational tools to analyze the underlying nonlinear behavior. Today, physical/analogical models are still basilar for the learning and experimenting process of form-made structures, because of the intuitive understanding that they can provide (Salvadori and Tempe 1983). Meanwhile, they are also a mean to emphasize the correlation between form and structural behavior (Hilson 1993) and to explore innovative designs (Royer-Carfagni 1999). The set of the most various performative forms can then be refined and selected from model to model. For example, the natural wrinkling of tensioned membrane can also inspire increased design possibilities for cable nets following an underlying optimal criterion, because wrinkles are the effect of the attempt of the membrane to respond to external loads by reorienting itself, specifically by *maximizing* the extensional stiffness. In a wrinkled region, the tensile stress is uniaxial in the direction of the wrinkles, so that one can think of an optimally-stiff cable arrangement following the same directions (Royer-Carfagni 1999; Barsotti et al. 2001).

With the development of computer graphic, novel design methods have been developed that address the nonlinear problem of the design of cable systems by reinterpreting old graphical methods. For example, Beghini et al. (2013) used graphic static to formulate solutions for cable nets made of primary and secondary cables. An analogy with the behavior of isotropic material was introduced by Cai (2011) for studying the topology optimization of tension structures, yet it does not produce a significant reduction in the time and computation effort.

A soap film naturally achieves a minimal-surface configuration. This can help to define the optimal shape of membranes and, by analogy, of cable nets, under a uniform equibiaxial state of stress, but no geometric transformation can be obtained by uniformly varying the stress: if one neglects the effects of the self-weight and external loads, the shape would substantially remain the same if the membrane is further uniformly stretched, even if the stiffness is modified. In order to modify the surface while maintaining fixed the position of the border, it is necessary that the stress is not any more equibiaxial. In fact, since the stress and curvature in one direction is related with the stress and curvature in the orthogonal direction, it is not the tension level, but the ratio between the tensions in the two directions, that can change the equilibrium configuration. Unfortunately, soap films cannot reproduce the response of structures that are unevenly stressed. However, we will demonstrate the following analogy between changes in input boundary and changes in input tension under the kinematic hypothesis of small strains and large rotations. Suppose that the surface $w(x,y)$: $\Omega \subset \mathbb{R}^2 \rightarrow \mathbb{R}$ represents the (uniform equibiaxial) equilibrium configuration of a soap film. If the corresponding geometric surface is *graphically* stretched under a linear scale transformation, different in the x and y directions, one obtains the equilibrium shape of a membrane that is differently tensioned in the in the x and y directions. Using standard software, it is easy to stretch a digital photograph of a soap film surface and thus obtain an immediate visual representation of the shape of the non-uniformly tensioned membrane.

This rationale can be used in a generative procedure. Since the resulting shapes derive from the geometric stretching of a soap film surface, this approach somehow represents the extension to the case of unevenly stressed tensile structures of the optimal configuration deduced through the physical model. According to Shea et al. (2005), generative design consists in creating new design processes that produce spatially novel, yet efficient and buildable, designs through exploitation of current computing and manufacturing capabilities. On the other hand, Frazer (1995) describes it as a complex growth process to transform an encoded seed into a design, enhancing the idea of target explorations as a consequence of using a fast design algorithm. This latest definition is particularly suitable for the proposed method, because here a generic minimal surface of desired boundary can be used as the starting point for a speculative form finding process of the transformations occurring into a membrane, or a cable net, by varying its tension. To this respect, the present work is somehow related with a recent

study on transformable membranes (Beatini and Royer-Carfagni 2016), where the transformation capabilities of quasi-developable tensioned membranes were investigated.

While implementing the method, we have successfully compared the results with those obtainable with the freeware parametric plug-in Grasshopper™ and RhinoMembrane© within the supporting Rhino© software, which allows to define minimal energy configurations of cable nets once the boundary conditions are given. Parametric modeling is a mute tool that involves "the use of geometric constraints as well as dimensional relations and data to drive shape definition" (Aish 1992). After all, the definite step-change that is making accessible quality experimentations outside from the great intuition of masters as Otto or Gaudi is the parametric design environment (Lynn 1993), into which most often the generative design is considered to operate (Szalapaj 2001). However, although the parametric environment allows for increased speed and accuracy, indeed the physical model is more intuitive.

The presented study uses minimal surfaces and their stretched images as molding tools that allow investigating structurally informed design options, in line with other structurally performative based generative designs (Rippmann et al. 2012; Adriaenssens et al. 2014; Menges 2012). The method could be used to conceive transformable membranes and cable nets, structures that can change their shape by modifying the ratio between the tensile stress in the warp and weft directions. Indeed, structures able to change their characteristics are enviable, and advances in technologies are making them realistic and real. We may cite, as examples, the prototypes of smart shells that can adapt to various external loads through minor shape adjustments (Schittich et al. 2013), or the proposals for proper transformable architecture that changes to fit different spaces (Beatini 2015a, b; Tachi 2010; Gantes 2001). The transformable cable net design method here presented not only highlights the increased possibilities of transformation, but it is also a more intuitive, directly manageable approach to form finding.

2 The model

Consider a membrane, initially planar in its undistorted reference state, in which the state of stress is homogeneous but not uniform equibiaxial, i.e., the two principal components of stress do not vary from point to point, but can be substantially diverse one another. In a possible analogy with cable nets, this condition can be achieved when the undistorted reference configuration is planar and made by two orthogonal families of parallel straight cables, when one family is tensioned differently from the other and, after the deformation, the cables of the two families remain *almost* orthogonal one another. If the number of cables is sufficiently high and their distances is sufficiently small, the set of cables can be homogenized (Royer-Carfagni 2003) and a continuum-theory description can be adopted for the corresponding Representative Volume Element (RVE). For convenience, in the following we will refer to membranes that might be considered also to be derived from this kind of homogenized cable nets.

A reference system (x,y,z) is chosen such that the axes x and y are parallel to the cords. Let then $\Omega(x,y) \subset \mathbb{R}^2$ represent the (homogenized) undistorted reference of the membrane/cable net, and let $u(x,y)$, $v(x,y)$ and $w(x,y)$ represent the components of displacement of a particle, initially at $(x,y,0)$, in the direction of the axes x, y, and z, respectively.

2.1 Variational approach and governing equations

The in-plane components of the Green-Lagrange strain associated with a distortion of the cable net take the form

$$\begin{aligned} e_{xx} &= \frac{1}{2}\left[\left(1+u_{,x}\right)^2 + v_{,x}^2 + w_{,x}^2 - 1\right] \ , \\ e_{yy} &= \frac{1}{2}\left[\left(1+v_{,y}\right)^2 + u_{,y}^2 + w_{,y}^2 - 1\right] \ , \\ e_{xy} &= \frac{1}{2}\left[\left(1+u_{,x}\right)u_{,y} + \left(1+v_{,y}\right)v_{,x} + w_{,x}w_{,y}\right] \ , \end{aligned} \tag{2.1}$$

where the comma denotes partial differentiation with respect to the variable indicated afterwards, e.g., $u_{,x} \equiv \frac{\partial u}{\partial x}$. If ε represents an order parameter of smallness, let us suppose that $w_{,x} = \mathrm{O}(\varepsilon)$ and $w_{,y} = \mathrm{O}(\varepsilon)$ and that $u_{,x} = \mathrm{o}(\varepsilon)$, $u_{,y} = \mathrm{o}(\varepsilon)$, $v_{,x} = \mathrm{o}(\varepsilon)$, $v_{,y} = \mathrm{o}(\varepsilon)$. Thus if one neglects, according to the classical von Kármán theory of plates, terms of order higher than ε^2, then (2.1) becomes

$$\begin{aligned} e_{xx} &= u_{,x} + \frac{1}{2}w_{,x}^2 \ , \\ e_{yy} &= v_{,y} + \frac{1}{2}w_{,y}^2 \ , \\ e_{xy} &= \frac{1}{2}\left[u_{,y} + v_{,x} + w_{,x}w_{,y}\right] \ . \end{aligned} \tag{2.2}$$

Supposing that the system has some stiffness with respect to the shear deformations e_{xy}, assuming that the axes x and y are of elastic symmetry, the homogenized material results to be elastic orthotropic, and the constitute equations result of the form

$$\begin{aligned} \sigma_{xx} &= \frac{E_x}{1-\nu_x\nu_y}\left(e_{xx} + \nu_y \ e_{yy}\right) \ , \\ \sigma_{yy} &= \frac{E_y}{1-\nu_x\nu_y}\left(e_{yy} + \nu_x \ e_{xx}\right) \ , \\ \tau_{xy} &= 2G \ e_{xy} \ , \end{aligned} \tag{2.3}$$

where E_x, E_y, $\nu_x/E_x = \nu_y/E_y$ and G are the elastic parameters of the orthotropic material. In the simplest case in which the membrane has negligible shear stiffness, as it is the case in which it is the homogenized view of a net of orthogonal cables, one can assume that $\nu_x/E_x = \nu_y/E_y = G \cong 0$, so that

$$\begin{aligned}\sigma_{xx} &= E_x e_{xx},\\ \sigma_{yy} &= E_y e_{yy}\ ,\\ \tau_{xy} &= 0\ .\end{aligned} \tag{2.4}$$

For this particular case, denoting with A_x and A_y, and with i_x and i_y, the area of each cable and the corresponding axial distance for cables parallel to the x and y axes, respectively, one has

$$E_x = \frac{A_x}{i_x\ s}E, \qquad E_y = \frac{A_y}{i_y\ s}E\ , \tag{2.5}$$

where E is the Young's modulus of each cable, supposed constant, and s is the reference thickness for the equivalent membrane.

The general form of the elastic strain energy is

$$\Theta = \frac{s}{2}\int_\Omega \left[\frac{E_x}{1-\nu_x\nu_y}(e_{xx}+\nu_y e_{yy})e_{xx} + \frac{E_y}{1-\nu_x\nu_y}(e_{yy}+\nu_x e_{xx})e_{yy} + 4Ge_{xy}^2\right]dA \tag{2.6}$$

where the relationship between the displacement components u, v and w and the strain components e_{xx}, e_{yy}, e_{xy} is given by (2.2). We suppose that, in the reference state Ω, traction forces per unit area of components t_x, t_y and t_z are applied on the part $\partial_t\,\Omega$ of the membrane border $\partial\Omega$, whereas on the complementary part $\partial_u\,\Omega = \partial\Omega\backslash\partial_t\,\Omega$ the displacement components

$$u=\overline{u},\quad v=\overline{v},\quad w=\overline{w}\ ,\quad \forall (x,y)\in\partial_u\Omega\ , \tag{2.7}$$

are prescribed. The total energy functional thus reads

$$\begin{aligned}\Pi = &\frac{s}{2}\int_\Omega \left[\frac{E_x}{1-\nu_x\nu_y}(e_{xx}+\nu_y e_{yy})e_{xx} + \frac{E_y}{1-\nu_x\nu_y}(e_{yy}+\nu_x e_{xx})e_{yy} + 4Ge_{xy}^2\right]dA\\ &+ -s\int_{\partial_t\Omega}\left(t_x u + t_y v + t_z w\right)\ dl\end{aligned} \tag{2.8}$$

Taking the first variation of this functional with respect to the variations $u+\delta u$, and $v+\delta v$, one obtains the field equations

$$\begin{aligned}\sigma_{xx,x}+\tau_{xy,y} &= 0, \quad \forall (x,y)\in\Omega,\\ \tau_{xy,x}+\sigma_{yy,y} &= 0, \quad \forall (x,y)\in\Omega,\end{aligned} \tag{2.9}$$

together with the natural boundary conditions

$$\begin{aligned}\sigma_{xx}n_x+\tau_{xy}n_y &= t_x\ ,\quad \forall (x,y)\in\partial_t\,\Omega,\\ \tau_{xy}n_x+\sigma_{yy}n_y &= t_y\ ,\quad \forall (x,y)\in\partial_t\,\Omega,\end{aligned} \tag{2.10}$$

where n_x and n_y denote the components of the outer unit normal to $\partial\Omega$ in the (x,y) plane. Taking the variation $w+\delta w$, the first variation of (2.8) gives

$$\begin{aligned}\delta\Pi_w = &\frac{s}{2}\int_\Omega \left[\sigma_{xx}w_{,x}\ \delta w_{,x} + \sigma_{yy}w_{,y}\ \delta w_{,y} + \tau_{xy}\left(w_{,x}\ \delta w_{,y} + w_{,y}\ \delta w_{,x}\right)\right]dA\\ &+ -s\int_{\partial_t\Omega} t_z\ \delta w\ dl = 0\end{aligned} \tag{2.11}$$

which, considering (2.9), implies

$$\sigma_{xx}w_{,xx} + 2\tau_{xy}w_{,xy} + \sigma_{yy}w_{,yy} = 0\ ,\quad \forall (x,y)\in\Omega\ , \tag{2.12}$$

and the boundary condition

$$\begin{aligned}&\left(\sigma_{xx}w_{,x}+\tau_{xy}w_{,y}\right)n_x + \left(\tau_{xy}w_{,x}+\sigma_{yy}w_{,y}\right)n_y = t_z,\\ &\forall (x,y)\in\partial_t\Omega.\end{aligned} \tag{2.13}$$

In conclusion, the boundary value problem is completely defined by the equilibrium (2.9) and (2.12), the compatibility (2.2), the constitutive (2.3) and the boundary conditions (2.7), (2.10) and (2.13). In particular, (2.12) represents the equilibrium in the z direction of an elementary portion of the membrane.

2.2 Geometric analogy of transformable equilibrium states

It is clear that in this theory, where the strains are given by (2.2), the curvatures are approximated with the second derivatives of the out-of-plane displacement $w(x,y)$, so that the components of the curvature tensor $1/R_x$, $1/R_y$, $1/R_{xy}$ take the form

$$\frac{1}{R_x}\cong w_{,xx},\quad \frac{1}{R_y}\cong w_{,yy}\ ,\quad \frac{1}{R_{xy}}\cong w_{,xy} \tag{2.14}$$

More in general, if x' and y' denote a new reference system such that β and $\beta+\pi/2$ are angles that x' and y' form with the x axis respectively, one has that

$$\begin{aligned}w_{,xx} &= w_{,x'x'}\cos^2\beta - 2w_{,x'y'}\sin\beta\cos\beta + w_{,y'y'}\sin^2\beta,\\ w_{,yy} &= w_{,x'x'}\sin^2\beta + 2w_{,x'y'}\sin\beta\cos\beta + w_{,y'y'}\cos^2\beta,\\ w_{,xy} &= \left(w_{,x'x'} - w_{,y'y'}\right)\sin\beta\cos\beta + w_{,x'y'}\left(\cos^2\beta - \sin^2\beta\right).\end{aligned} \tag{2.15}$$

Consequently, from (2.12) one finds

$$\begin{aligned}&\left(\sigma_{xx}\cos^2\beta + \sigma_{yy}\sin^2\beta + 2\tau_{xy}\sin\beta\cos\beta\right)w_{,x'x'}\\ &+ 2\left[\left(\sigma_{yy}-\sigma_{xx}\right)\sin\beta\cos\beta + 2\tau_{xy}\left(\cos^2\beta-\sin^2\beta\right)\right]w_{,x'y'}\\ &+ \left(\sigma_{xx}\sin^2\beta + \sigma_{yy}\cos^2\beta - 2\tau_{xy}\sin\beta\cos\beta\right)w_{,y'y'}\\ &= \sigma_{x'x'}w_{,x'x'} + 2\tau_{x'y'}w_{,x'y'} + \sigma_{y'y'}w_{,y'y'} = 0\end{aligned} \tag{2.16}$$

At each point (x,y), it is possible to define the principal directions of curvature, identified by the unit vectors $\mathbf{r}_1(x,y)$ and $\mathbf{r}_2(x,y)$, $\mathbf{r}_1(x,y)\cdot\mathbf{r}_2(x,y)=0$. If ξ and η denote the coordinate in a local reference frame (ξ,η) whose axes are parallel to $\mathbf{r}_1(x,y)$ and $\mathbf{r}_2(x,y)$ at each point (x,y), the principal curvatures $1/R_\xi$, $1/R_\eta$ read

$$\frac{1}{R_\xi} \cong w_{,\xi\xi}, \quad \frac{1}{R_\eta} \cong w_{,\eta\eta} \ , \quad \text{with} \quad \frac{1}{R_{\xi\eta}} \cong w_{,\xi\eta} = 0 \tag{2.17}$$

Thus, if x' and y' are made to coincide with ξ and η, one readily finds from (2.16) that

$$\sigma_{\xi\xi} w_{,\xi\xi} + \sigma_{\eta\eta} w_{,\eta\eta} = 0, \qquad \forall (\xi, \eta) \in \Omega \tag{2.18}$$

where $\sigma_{\xi\xi}$ and $\sigma_{\eta\eta}$ represent the normal components of stress in the direction of the axes ξ and η, respectively. Equivalently, if x' and y' now coincide with the principal directions of stress, say x^* and y^*, since $\tau_{x^* y^*} = 0$, one finds

$$\sigma_{x^* x^*} w_{,x^* x^*} + \sigma_{y^* y^*} w_{,y^* y^*} = 0 \ , \quad \forall \left(x^*, y^*\right) \in \Omega \tag{2.19}$$

The difference between (2.17) and (2.18) consists in the fact that the former is referred with respect to the principal direction of curvature, hence in general $\tau_{\xi\eta} \neq 0$, whereas in the latter the directions are those of principal stress, so that in general $w_{,x^* y^*} \neq 0$.

There is a simple but important case in which the principal directions of stress are immediately known, and this coincides with the condition in which $G \to 0$ in (2.3). Since the constitutive (2.4) hold, the axis x and y are parallel to the direction of principal stress in the whole membrane, and one has

$$\sigma_{xx} w_{,xx} + \sigma_{yy} w_{,yy} = 0 \ , \quad \forall (x, y) \in \Omega \tag{2.20}$$

In order to change the shape of the membrane one may imagine using devices, likewise hydraulic jacks, able to change the state of stress in two orthogonal direction.

Let us suppose that the configuration denoted with "0", associated with the state of stress $\sigma_{xx}^{(0)} = \sigma_{yy}^{(0)} = \sigma^{(0)}$ supposed *homogeneous* and uniformly equiabiaxial, produces the displacement field $w^{(0)}(x, y)$. This configuration is governed by the Laplace equation

$$w_{,xx}^{(0)} + w_{,yy}^{(0)} = 0 \ , \quad \forall (x, y) \in \Omega \tag{2.21}$$

and, as it is well known, it corresponds, within the approximation (2.14), to an "*optimal minimal surface*" configuration under the assigned boundary conditions. Such a configuration can be physically visualized for example by considering the deformation of a soap-film anchored to the boundary $\partial\Omega$ of Ω.

Let us now imagine to modify the state of stress into $\sigma_{xx}^{(1)}$ and $\sigma_{yy}^{(1)}$, supposed homogenous and constant in the membrane but *not* equibiaxial. Then (2.19) reads

$$\sigma_{xx}^{(1)} w_{,xx}^{(1)} + \sigma_{yy}^{(1)} w_{,yy}^{(1)} = 0 \ , \quad \forall (x, y) \in \Omega \tag{2.22}$$

so that $w^{(1)}(x, y)$ is not any more associated with a minimal surface.

However, one can make the change of variables

$$\tilde{x} = a_x x + c_x, \quad \tilde{y} = a_y y + c_y, \tag{2.23}$$

where a_x, a_y, c_x and c_y are constants, so that the domain Ω is transformed in the domain $\tilde{\Omega}$. Since clearly

$$w_{,xx}^{(1)} = a_x^2 w_{,xx}^{(1)} \ , \qquad w_{,yy}^{(1)} = a_y^2 w_{,yy}^{(1)} \ , \tag{2.24}$$

one has from (2.21) that

$$\sigma_{xx}^{(1)} a_x^2 w_{,xx}^{(1)} + \sigma_{yy}^{(1)} a_y^2 w_{,yy}^{(1)} = 0 \ , \quad \forall \left(\tilde{x}, \tilde{y}\right) \in \tilde{\Omega} \tag{2.25}$$

It is then sufficient to choose a_x and a_y such that

$$\sigma_{xx}^{(1)} a_x^2 = \sigma_{yy}^{(1)} a_y^2 \ , \tag{2.26}$$

to obtain again the Laplace equation

$$w_{,xx}^{(1)} + w_{,yy}^{(1)} = 0 \ , \quad \forall \left(\tilde{x}, \tilde{y}\right) \in \tilde{\Omega} \tag{2.27}$$

The importance of (2.22)–(2.26) consists in the fact that they represent a geometric analogy that correlates a change of stress with a geometric deformation of the boundary. By using the transformation (2.22), one obtains under the condition (2.25) the Laplace equation, i.e., the cable net takes the form of a minimal surface. The form of the resulting surface can be obtained either analytically or, more interestingly, using the soap film analogy.

One this shape has been determined, it is the sufficient to go back to the domain Ω by setting

$$x = \left(\tilde{x} - c_x\right) \Big/ a_x, \quad y = \left(\tilde{y} - c_y\right) \Big/ a_y, \quad (x, y) \in \Omega \tag{2.28}$$

This is equivalent to geometrically stretching the surface so determined so that it fits back in domain Ω.

A few examples, presented in the following section, will contribute to clarify the method.

3 Generative form-finding from minimal surfaces

Our aim here is to use the geometric analogy presented in Section 2.2 to provide the generative design for membranes under an orthotropic stress state by means of physical models.

3.1 The physical representation with soap-films

Under the hypotheses of the model of Section 2, the Laplace equation (2.21) with appropriate Dirichlet boundary conditions defines the minimal surface $w = w^{(0)}(x,y)$, $(x,y) \in \Omega$, such that $w = \overline{w}^{(0)}(x, y)$ on the boundary $(x,y) \in \partial\Omega$. This is the optimal shape assumed by the membrane when the state of stress is uniform equibiaxial, i.e., $\sigma_{xx}^{(0)} = \sigma_{yy}^{(0)} = \sigma^{(0)}$. A physical approach to represent such a surface consists in shaping an iron wire so to reproduce the boundary $w = \overline{w}^{(0)}(x, y)$, $(x,y) \in \partial\Omega$, and forming across it a soap film surface with zero excess

pressure. If the state of stress in the membrane is not equibiaxial, no soap film can reproduce the corresponding shape assumed by the membrane. However, one can use the geometric method defined by (2.23)–(2.28).

To illustrate the procedure with a practical example, let Ω be the square domain $|x|+|y| \le d$, with a piecewise linear boundary defined by the heights of the corner points $\overline{w}^{(0)}(d,0) = \overline{w}^{(0)}(-d,0) = 2h$ and $\overline{w}^{(0)}(0,d) = \overline{w}^{(0)}(0,-d) = 0$. Within the hypothesis (2.14), the minimal optimal surface is approximated by a hyperbolic paraboloid (hypar) represented by the equation

$$\overline{w}^{(0)}(x,y) = \left[\left(x/d\right)^2 - \left(y/d\right)^2 + 1\right] h \ , \qquad (x,y)\in\Omega \ . \tag{3.1}$$

Suppose that now we are interested in finding the shape assumed by the membrane when the state of stress is homogeneous but not any more equibiaxial, represented by $\sigma_{xx} = \sigma_{xx}^{(1)}$ and $\sigma_{yy} = \sigma_{yy}^{(1)}$. The strategy is to stretch the boundary according to the transformation (2.23), by selecting the parameters a_x and a_y such that (2.26) holds (the parameters c_x and c_y are inessential for this construction and can be set equal to zero, without losing generality). Therefore, there are many ways to select such a transformation. One may assume for example that $a_y = 1$ and find the corresponding a_x from (2.26) as $a_x = \sqrt{\sigma_{yy}^{(1)}/\sigma_{xx}^{(1)}}$. This is equivalent to stretching the boundary only in the direction of the x axis. One can also perform a transformation such that each of the linear pieces forming the boundary maintain unaltered their lengths, and in this way one readily obtains

$$a_x = \sqrt{\frac{2\ \sigma_{yy}^{(1)}}{\sigma_{xx}^{(1)} + \sigma_{yy}^{(1)}}} \ , \qquad a_y = \sqrt{\frac{2\ \sigma_{xx}^{(1)}}{\sigma_{xx}^{(1)} + \sigma_{yy}^{(1)}}} \ . \tag{3.2}$$

This means that the reference domain Ω, initially square, is distorted to the rhombus $\tilde{\Omega}$ without changing the length of the sides.

At this point, one can construct the "minimal" surface associated with $\tilde{\Omega}$, with conditions $\overline{w}^{(1)}(\pm a_x d, 0) = 2h$ and $\overline{w}^{(1)}(0, \pm a_y d) = 0$, which turns out to be the hypar

$$\overline{w}^{(1)}\left(\tilde{x},\tilde{y}\right) = \left[\left(\frac{\tilde{x}}{d}\right)^2 - \left(\frac{\tilde{y}}{d}\right)^2 + a_y^2\right] \frac{2h}{a_x^2 + a_y^2} \quad , \qquad \left(\tilde{x},\tilde{y}\right)\in\tilde{\Omega} \ . \tag{3.3}$$

A physical way to visualize such a surface consists, again, in forming a new soap film with zero overpressure across the boundary $\partial\tilde{\Omega}$.

The final step is to return back to the domain Ω by applying (2.28). In this way one finds

$$\begin{aligned} \overline{w}^{(1)}(x,y) &= \left[\left(\frac{a_x x}{d}\right)^2 - \left(\frac{a_y y}{d}\right)^2 + a_y^2\right] \frac{2h}{a_x^2 + a_y^2} \\ &= \left[\sigma_{yy}^{(1)}\left(\frac{x}{d}\right)^2 - \sigma_{xx}^{(1)}\left(\frac{y}{d}\right)^2 + \sigma_{xx}^{(1)}\right] \frac{2h}{\sigma_{xx}^{(1)} + \sigma_{yy}^{(1)}} \quad , \quad (x,y)\in\Omega. \end{aligned} \tag{3.4}$$

It is immediate to check that this surface verifies (2.22). Remarkably, that equation holds whatever the value of the parameter h.

An example with soap films is represented in Figs. 1 and 2. Figure 1a represents the minimal surface obtained with an unpressurized soap film connecting a piecewise linear boundary defined in the reference domain Ω. Introducing the reference system with the x (y) axis parallel to the line connecting the two highest (lowest) points, now apply the transformation (2.23) with $a_y = 1$ and $a_x > 1$ to reach the stretched domain $\tilde{\Omega}$. The resulting minimal surface is represented in Fig. 1b, where

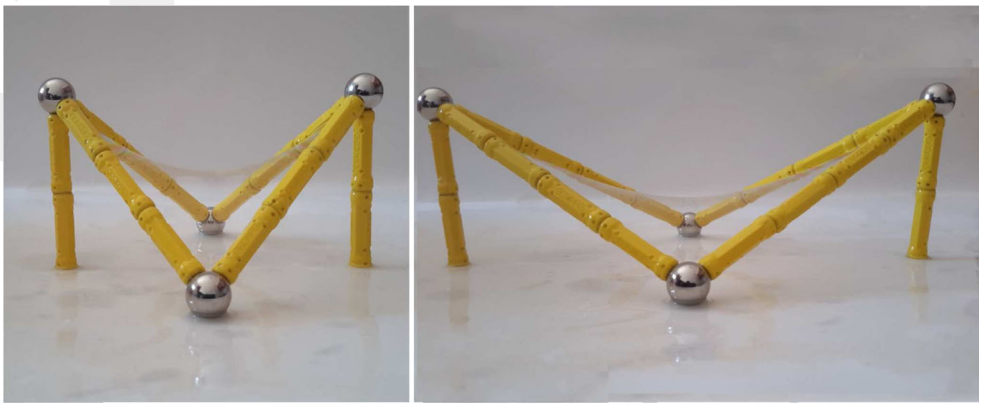

a **b**

Fig. 1 (**a**) Minimal surface obtained with a soap film in the reference domain Ω. (**b**) Minimal surface in the stretched domain $\tilde{\Omega}$, obtained with $a_x > 1$ and $a_y = 1$

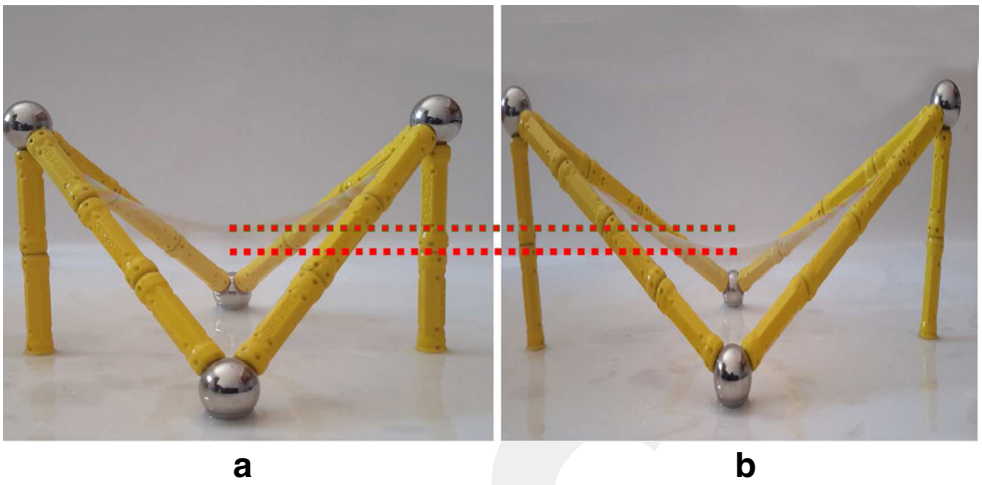

Fig. 2 Comparison of the minimal surface obtained in the domain Ω (**a**) and (**b**) the surface that is obtained by geometrically stretching back to Ω the minimal surface obtained in the domain $\tilde{\Omega}$ (with $a_x > 1$ and $a_y = 1$)

the difference with Fig. 1a is clear by counting the number of sticks that compose the frame.

Figure 2 shows the comparison between the minimal surface constructed in the domain Ω (Fig. 2a), the same of Fig. 1a, with the surface (Fig. 2b) that is obtained by scaling back to Ω the minimal surface obtained in Fig. 1b in the domain $\tilde{\Omega}$, according to (2.28). Now the surface is again defined on Ω, and since the value of h in (3.3) is arbitrary, one has obtained a surface that verifies (2.22) and respects the original boundary conditions.

It is evident that the resulting (anisotropically stressed) membrane is lower than the minimal surface configuration of a (uniform equibiaxially stressed) soap film. In fact, in the construction $a_x = \sqrt{\sigma_{yy}^{(1)}/\sigma_{xx}^{(1)}} > 1$, so that $\sigma_{yy}^{(1)} > \sigma_{xx}^{(1)}$. The resulting shape is thus in agreement with the physical intuition: if the membrane is more stressed in the direction y than in the direction x, it is clear that the fibers are tauter in the direction y that in the direction x, and therefore the corresponding curvature is lower.

This example illustrates the feasibility of the proposed method. It is easy, in fact, using a simple image editor, to stretch a digital picture of the isotropically stressed membrane of Fig. 1b to obtain the "distorted" image of Fig. 2b. The surface in this picture represents the configuration of an orthotropically stressed membrane, whose state of stress is associated with the distortion parameters a_x and a_y through (2.26).

The method just presented has been verified with digital models for the case of cable nets, which may be considered an approximation of membrane structures. Given a non-tensioned structure, defined in the reference planar domain Ω, the target structure under a non-uniform stress is achieved with a three-step procedure. Firstly, the domain Ω and so the boundary conditions for the cable net, are geometrically stretched into $\tilde{\Omega}$ according to (2.22). Secondly, a form finding process under constant prestress is performed. Finally, the tensioned surface so obtained is geometrically scaled back to the original domain Ω, simply reversing the scale factor applied in step one. It should be emphasized that this procedure allows obtaining pretensioned structures under anisotropical prestress without dealing with their direct form finding process. Indeed, anisotropic prestress would be very unpractical to be physically simulated; meanwhile, if performed digitally, it would require a deep evaluation of available form-finding processes, as well as of their setting parameters.

The physical models are made by composing the boundary with magnetic modular rigid bars, each 4cm long, and soap water films. The digital models are obtained through the user-friendly plug-ins Grasshopper™ and RhinoMembrane© within the Rhino© CAD environment. Grasshopper™ is a parametric design software, used here to create the reference geometry of the nets. RhinoMembrane© plug-in finds the equilibrated forms of those nets and has been chosen among other options

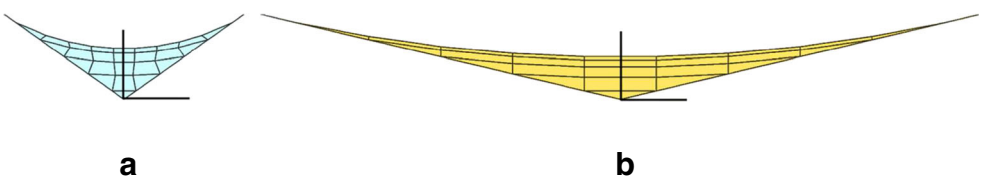

Fig. 3 (**a**) Minimal energy cable net in the domain Ω, calculated in the Grasshopper™ environment. (**b**) Minimal cable net in the in the stretched domain $\tilde{\Omega}$, obtained with $a_x > 1$ and $a_y = 1$

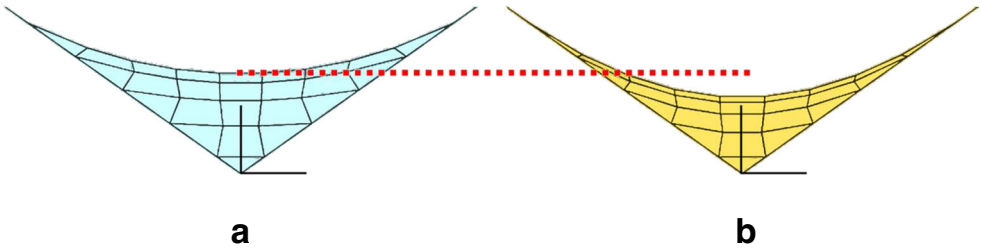

Fig. 4 Comparison of the minimal cable net obtained in the domain Ω (**a**) and (**b**) the surface that is obtained by scaling back to Ω the minimal surface obtained in the domain $\tilde{\Omega}$, having set $a_x > 1$ and $a_y = 1$

(Kangaroo, Karamba, etc.) because it provides, as an option, a form finding procedure that minimizes the energy of the cable nets.

Indeed, the software uses a generalization of the well-known "force density method" originally developed in (Sheck 1974). The force density is the ratio of stress over cable length; the solution corresponding to the case of constant force densities is associated with the minimization of the squared sum of length between consecutive points. More precisely, the method implemented in the software is the so called "Updated Reference Strategy" (Bletzinger and Ramm 1999), which allows reproducing also the shape of membranes thanks to an iterative procedure. As noted by the developer, the two methods actually coincide for cable nets.

Figure 3 represents the counterpart of Fig. 1 when the minimal surface is directly calculated for a net of orthogonal cables using the parametric environment of Grasshopper™, either in the reference domain Ω or in the stretched domain $\tilde{\Omega}$, setting in the transformation (2.23) $a_x > 1$ and $a_y = 1$ according to (2.26). The shape has been calculated by the program following the configuration of minimal energy (force density method). Figure 4 represents the comparison between the minimal energy configuration of the cable net in the domain Ω, and the configuration that is obtained with the position (2.28), scaling back from $\tilde{\Omega}$ to Ω. The stretching of the geometry can be readily obtained within the computer program. The results are in agreement with the shapes obtained with the soap bubbles.

Figure 5 represents the comparison of the results of the physical models with the Grasshopper™ analysis. Results are in excellent agreement.

In conclusion, the method that has just been outlined allows determining shapes of unevenly stressed cable nets. The novelty consists in the physical model that extends to this case the soap bubble analogy, simply using a geometrical stretching of digital images.

3.2 Further examples of tension induced transformations

The same procedure outlined in the previous section can be repeated to represent the effects of varying the state of stress in membranes/cable nets when the boundary if of a higher degree of complexity. For the reference domain Ω, Fig. 6a shows a soap film that joins two arches and takes the shape of a catenoid. The arches are further pulled apart one from the other while passing to the domain $\tilde{\Omega}$ in the coordinate change (2.23), by setting $a_y = 1$ and $a_x = \sqrt{\sigma_{yy}^{(1)}/\sigma_{xx}^{(1)}} > 1$, and the new soap surface is represented in Fig. 6b. Figure 7 shows the comparison of the catenoid associated with Ω with the shape found by scaling back from $\tilde{\Omega}$ to Ω, according to (2.28). As expected, the longitudinal profile lowers, i.e., the catenary becomes more arched, because $a_x = \sqrt{\sigma_{yy}^{(1)}/\sigma_{xx}^{(1)}} > 1$, implies $\sigma_{yy}^{(1)} > \sigma_{xx}^{(1)}$, which means that the transversal overstressed fibers pulls down the longitudinal fibers.

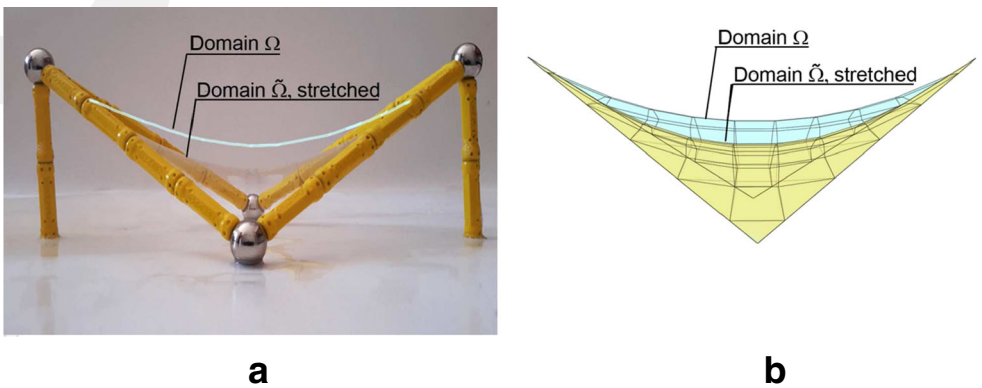

Fig. 5 (**a**) Surface obtained by stretching back to Ω the soap film obtained in the domain $\tilde{\Omega}$ and comparison with the profile in the domain Ω. (**b**) Comparison of the optimal cable net in the domain Ω and the cable configuration obtained by stretching back from $\tilde{\Omega}$ to Ω. Parameters a_x and a_y from (3.2)

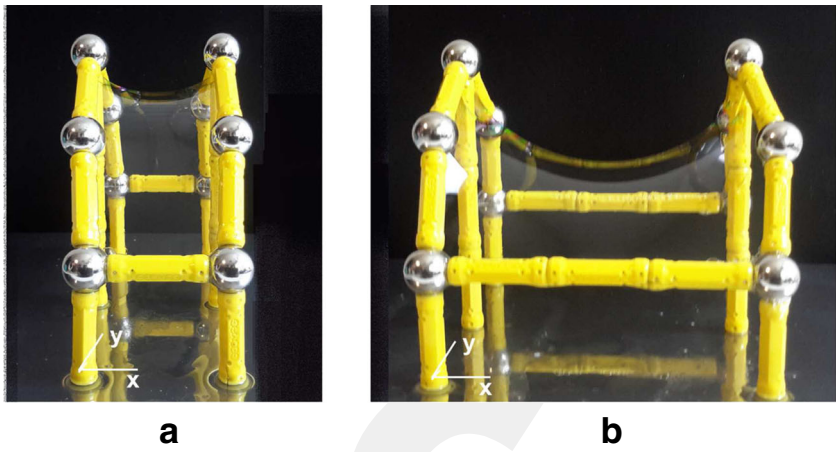

Fig. 6 (**a**) Catenoid joining two arches in the reference domain Ω. (**b**) Catenoid in the stretched domain $\tilde{\Omega}$ (obtained with $a_x > 1$ and $a_y = 1$)

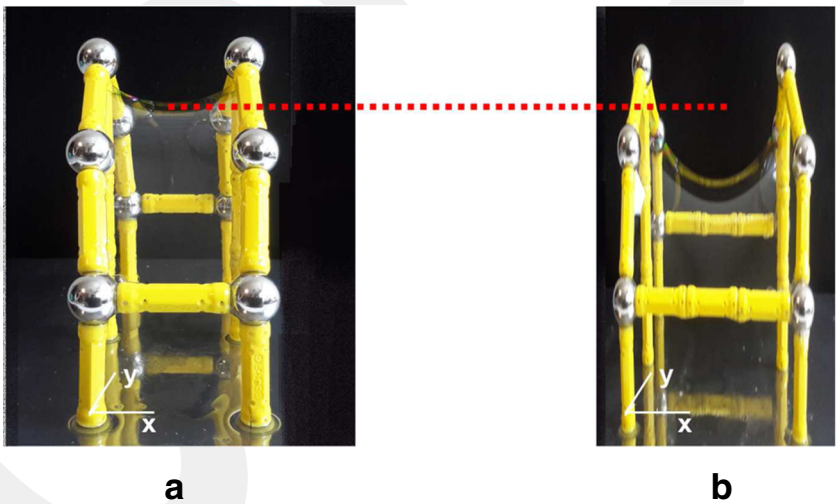

Fig. 7 Comparison of the soap film obtained in the domain Ω (**a**) and the surface obtained by scaling back to Ω the soap film in the domain $\tilde{\Omega}$ (with $a_x > 1$ and $a_y = 1$)

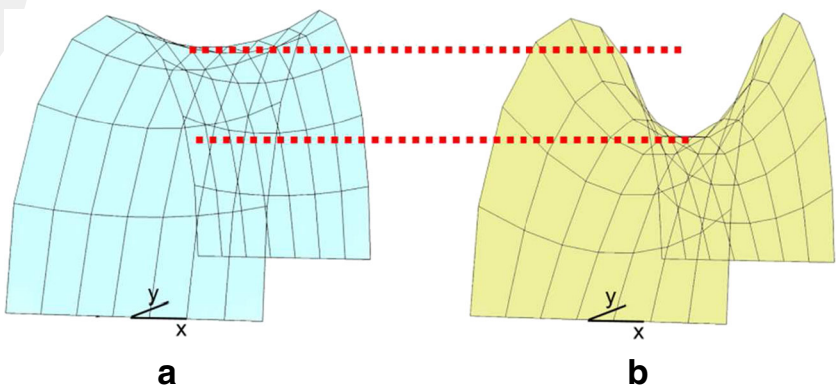

Fig. 8 Comparison of the minimal cable net surface obtained in the domain Ω (**a**) and (**b**) the surface obtained by stretching back to Ω the minimal cable net in the domain $\tilde{\Omega}$ (with $a_x > 1$ and $a_y = 1$)

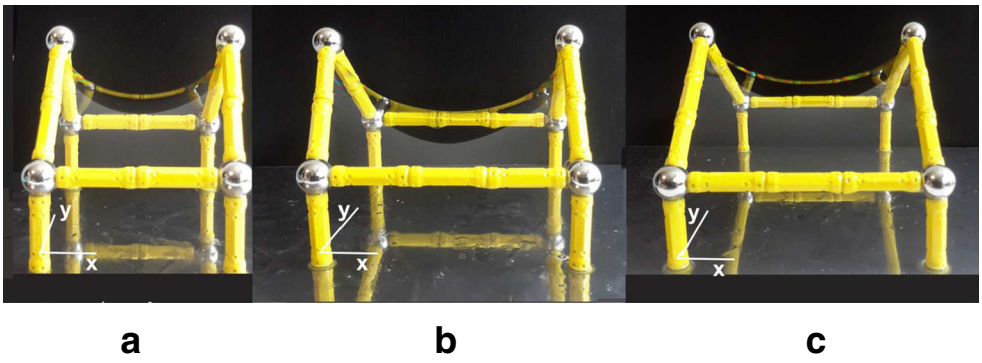

Fig. 9 (**a**) Gable-like soap film in the reference domain Ω. (**b**) Gable-like soap film in the stretched domain $\tilde{\Omega}$ obtained with $a_x > 1$ and $a_y = 1$. (**c**) Gable-like soap film in the stretched domain $\tilde{\Omega}$ obtained with $a_x > 1$ and $a_y > 1$

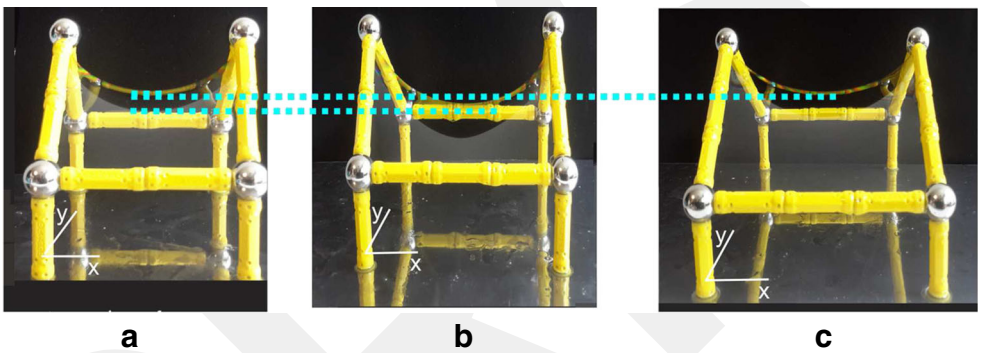

Fig. 10 Comparison of the soap film obtained in the domain Ω (**a**) and the surfaces obtained by stretching back to Ω in one direction the soap film of $\tilde{\Omega}$ (with $a_x > 1$ and $a_y = 1$) (**b**) and by stretching back in two directions the soap film of $\tilde{\Omega}$ (with $a_x > 1$ and $a_y > 1$) (**c**)

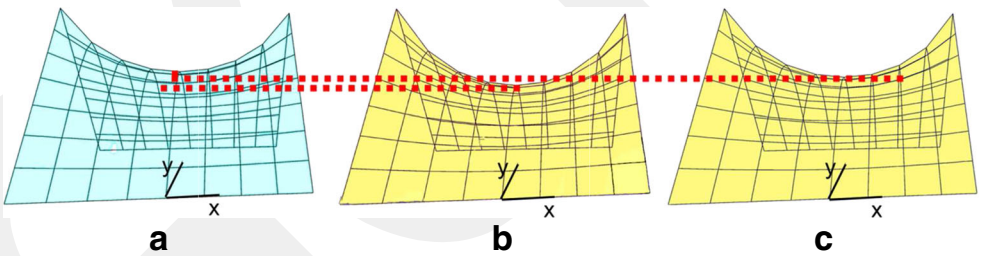

Fig. 11 Comparison of the minimal cable net obtained in the domain Ω (**a**) and the surfaces obtained by stretching back to Ω in one direction the minimal cable net of $\tilde{\Omega}$ (with $a_x > 1$ and $a_y = 1$) (**b**), and by scaling back in two directions the minimal cable net of $\tilde{\Omega}$ (with $a_x > 1$ and $a_y = 1$) (**c**)

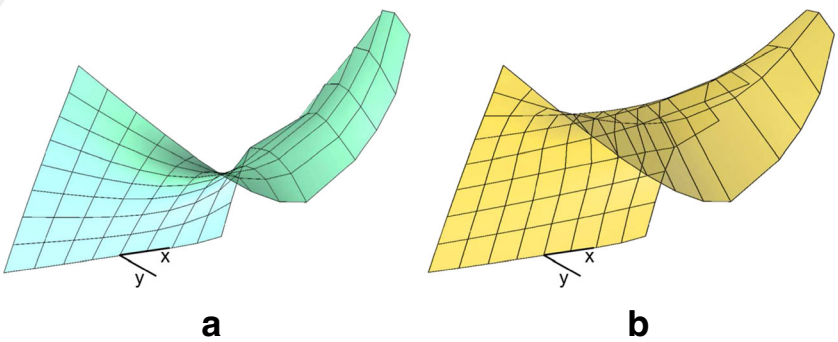

Fig. 12 (**a**) Minimal cable net obtained in the domain Ω. (**b**) Surface obtained by scaling back to Ω in one direction the minimal cable net of $\tilde{\Omega}$ (with $a_x = 1$ and $a_y > 1$)

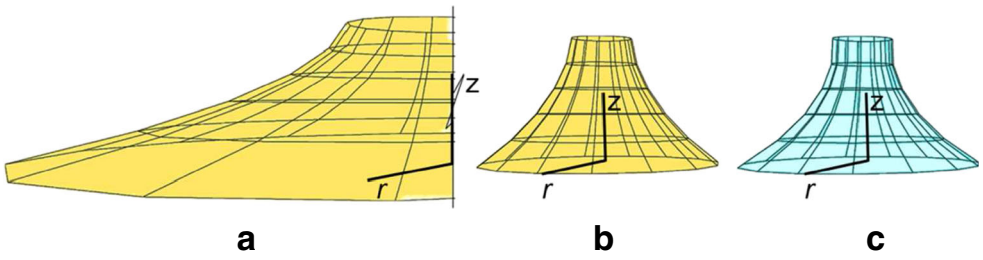

Fig. 13 (**a**) Minimal cable net in the stretched domain $\tilde{\Omega}$, obtained with obtained with $a_r > 1$. Comparison of the net obtained by stretching back to Ω the minimal cable net of $\tilde{\Omega}$ (**b**) and the minimal cable net in the domain Ω (**c**)

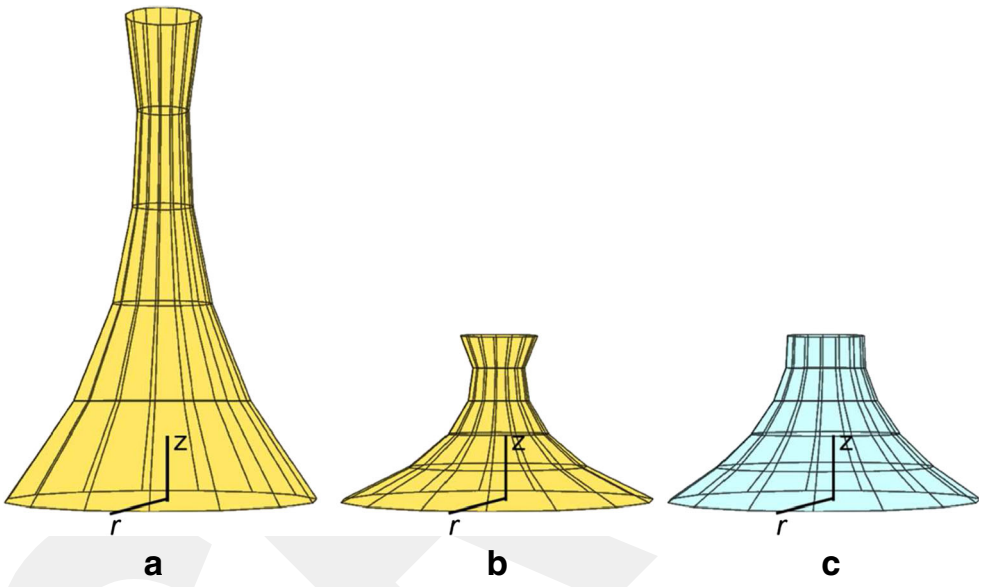

Fig. 14 (**a**) Minimal cable net obtained by maintaining fixed the domain Ω, and moving apart the circular boundaries along z. Surface obtain by moving back to the original height (**b**) and comparison with the corresponding minimal cable net (**c**)

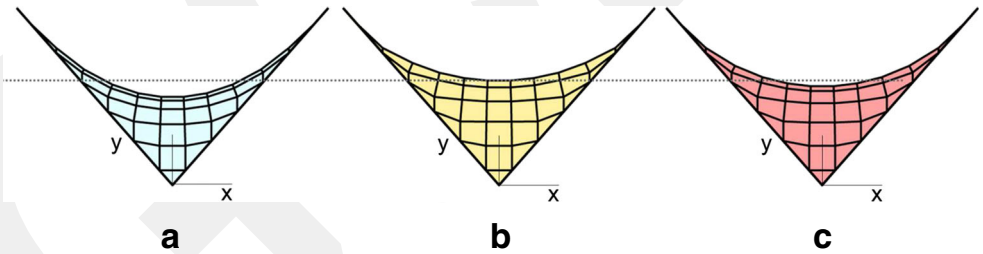

Fig. 15 (**a**) Cable net under a biaxial uniform prestress. (**b**) Cable net under anisotropic prestress, obtained with the presented procedure (with $a_x = 1$ and $a_y > 1$). (**c**) Cable net under the same anisotropic prestress, obtained with a force density form finding method (with $\sigma_{xx} > 1$ and $\sigma_{yy} = 1$)

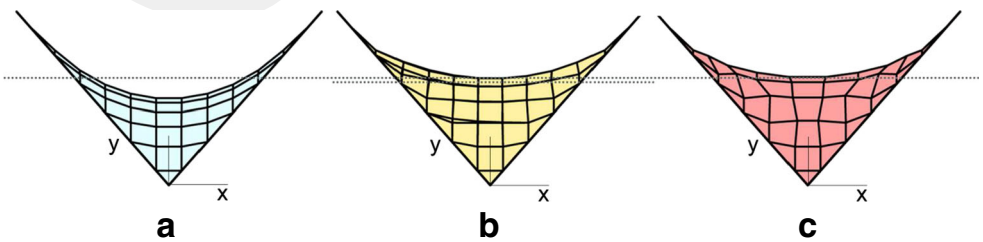

Fig. 16 (**a**) Membrane under uniform prestress. (**b**) Membrane under anisotropic prestress, obtained with the presented procedure (with $a_x = 1$ and $a_y > 1$). (**c**) Membrane under the same anisotropic prestress, obtained directly applying the updated force density method (with $\sigma_{xx} > 1$ and $\sigma_{yy} = 1$)

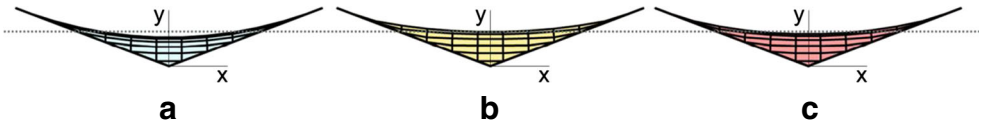

Fig. 17 (**a**) Cable net under a biaxial uniform prestress. (**b**) Cable net under anisotropic prestress, obtained with the presented procedure (with $a_x = 1$ and $a_y > 1$). (**c**) Cable net under the same anisotropic prestress, obtained with a force density form finding method (with $\sigma_{xx} > 1$ and $\sigma_{yy} = 1$)

Figure 8 repeats the same construction with cable nets using the parametric environment of Grasshopper™. Again the results are in perfect agreement with the construction of Fig. 7.

In the construction of Fig. 9 the construction is for a contouring frame that reproduces a gable roof. Counting the number of sticks, it is clear that in Fig. 9b the domain Ω has been stretched to $\tilde{\Omega}$ in x direction ($a_x > 1$ and $a_y = 1$), whereas in Fig. 9c the stretching is both in the direction of x and in the direction of y ($a_x > 1$ and $a_y > 1$). The forms that can be obtained by scaling back to the Ω are represented in Fig. 10.

Figure 11 indicates the analogous construction made with Grasshopper™. Comparison with Fig. 10 again demonstrates the possibilities of the parametric environment.

In fact, it is easy to use this simple computer program to analyze more complicated boundaries. Figure 12 refers to a free-form continuous boundary (two view points), where the stretching from Ω to $\tilde{\Omega}$ has been made according to $a_x > 1$ and $a_y = 1$.

Although not indicated in the analytical derivations of Section 2.2, the construction can be extended to the case of cable nets with rotational symmetries by using polar coordinates. For the case of Figure 13 the domain Ω is a circle. Figure 13a represents the minimal cable net in the domain $\tilde{\Omega}$, obtained by radial stretching of Ω (say, $a_r > 1$). Figure 13b indicates the net obtained by stretching back to Ω the minimal cable net obtained in $\tilde{\Omega}$. Comparison with the minimal cable net obtained in Ω can be obtained from Fig. 13c.

A similar-in-type analogy between soap films and cable nets can be obtained by considering further geometric transformations. For example, it would be possible also to maintain the domain Ω and to stretch the geometric figure in the direction z. A discussion similar in type to that performed in Section 2.2 allows establishing a correlation between the state of stress in the radial and circumferential cables. Just for the sake of illustration, Fig. 14a represents the minimal cable net that is obtained by maintaining fixed the domain Ω, and moving apart along z the two circular boundaries that define the membrane contours. Figure 14b denotes the surface obtained by moving back to the original height. The resulting surface is different from the one that could be obtained directly, represented in Fig. 14c.

These simple examples demonstrate that the potentialities of the method are yet to be fully investigated. The approach establishes a correlation through variations in the tensile stress and variations of the boundary and represents a form finding tools of very practical use.

3.3 Comparison with digital approaches

The theory underling the proposed method to approximate anisotropic states of stress has been demonstrated in Section 2, while Section 3.1 and 3.2 have presented its practical implementation. It could be interesting at this point to compare the results with the forms found by directly applying an anisotropic prestress to a structure defined within the desired domain. Obviously, we cannot simulate such process with physical models; therefore we just consider a digital form finding as discussed before, exploiting the capability of the software to simulate not only cable-nets, but also membranes. In the latest case, the force density method is iteratively applied by the software to take into account the peculiarities of membranes with respect to cable nets. A good convergence is found after 15 iteration steps.

Figure 15 illustrates a reference cable net under uniform prestress (a), the cable net found with the presented method (b) and finally a cable net under orthotropic prestress (c) with the ratio $\sigma^{(1)}_{yy}/\sigma^{(1)}_{xx} = 3$. According to the theory of Section 2, in Fig. 15b the values of the parameters a_x and a_y of (2.22) are set by applying (2.26), which gives in this case $a_x/a_y = \sqrt{3}$. Notice from the pictures that our method gives results that are in good agreement with the numerical finding. There is indeed a light difference, which should be attributed to the fact that the proposed method relies upon the von Kàrmàn representation of the membrane strain, which produces approximated strains for very large deformations, as in the case at hand.

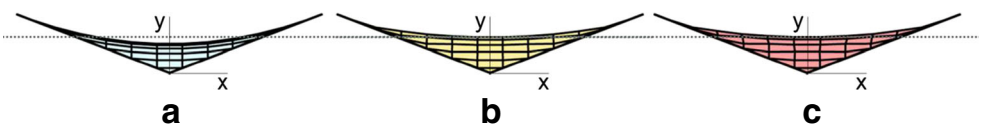

Fig. 18 (**a**) Membrane under uniform prestress. (**b**) Membrane under anisotropic prestress, obtained with the presented procedure (with $a_x = 1$ and $a_y > 1$). (**c**) Membrane under the same anisotropic prestress, obtained directly applying the updated force density method (with $\sigma_{xx} > 1$ and $\sigma_{yy} = 1$)

Figure 16 illustrates the same cases for a membrane under the same boundary condition of the cable net of Fig. 15. A shorter reference dot line is copied from Fig. 15 to highlight the difference in the results. As expected, the membrane has slightly different sag due to the in-plane shear effect, but in any case the proposed method result to be quite effective also for cable nets.

Figures 17 and 18 are equal in all to the previous two, except that for the boundary condition, as the contouring frame is much lower. As before, the dotted reference line of Fig. 17 has been copied in Fig. 18 (shorter line). In these cases, the differences between the anisotropically-stressed surfaces found with the software and with the presented method are hardly appreciable. In fact, for the present cases where the strains are much smaller, the approximation with the von Kàrmàn tensor is much more accurate.

4 Conclusions

We have proposed a generative form-finding algorithm for the design of orthotropically-stressed membranes, which relies upon an analogy with the minimal-surface configuration of soap films. The main result is certainly the established correspondence between the resulting shape and the surface obtained by geometrically stretching the natural minimal configuration of a soap film. Rules are given to relate the state of stress in the membrane with the geometric stretching of the soap film surface. It is then possible to offer an insight into the nonlinear behavior of tensioned structures in a simple and intuitive manner. Since a net of orthogonal cables can approximate the static state of an orthotropically stretched membrane, the construction here presented can also be extended to cable nets. The static state of an orthogonal patterned cable net can be varied by changing the tension in the warp direction with respect to the weft direction, and the method here proposed can be used to visualize the consequent transformations. From the analogy with soap films, it is then possible to offer an insight into the nonlinear behavior of tensioned structures in a simple and intuitive manner. Results have been successfully compared with the form-finding shapes obtained with the Grass hopper™ and RhinoMembrane© plug-in, within the Rhinoceros® software.

Of course, the construction of a transformable membrane or cable-net poses major problems, because the stress state must be changed. Fixed cable net facades have been proved to maintain acceptable deformation under external loads (Feng et al. 2009; Schlaich and Moschner 2005), but the active control of the tensioning system is the major problem. There are various examples of actuators applied to tendons for controlling the pre-stress under variable load conditions in bridges and decks (Preumont 2011; Fisco and Adeli 2011). The necessity to limit the displacements of the reflector surface of space mesh antennas is well known (Hedgepeth 1982). Recently various active systems have been developed for the truss like mesh antennas, the most common and advanced type: the reflecting mesh is attached to a front cable network having sinclastic surface and resisted by an equal and opposite rear surface cable net, the two being connected by boundary and tie cables. Control can be provided by activating the boundary cables or on the tie cables (Tanaka and Natori 2004). Springs are used in the configuration proposed by Lai and Pellegrino (2001), while in Wang et al. (2013) the tie cables are slightly shortened or lengthened by piezoelectric actuators. These technologies could be certainly transposed to the case at hand.

The relationship between the active cable net and the supporting structure should also be developed. Indeed, also the boundary could be modified to fit different shapes (Chen and You 2005; Beatini and Korkmaz 2013). Moreover, if the cable nets is the support of a façade or a roof, a particular type of envelope must be designed in such a way that it can comply with the net movements. Cable net structures have long been used in large roofs to support covering rigid panels (Buchholdt 1999). For example, in the Kempinski Hotel at Munich Airport, Schlaich, Bergermann und Partner successfully proposed cable networks to be used as a pure supporting structural system for a glass façade. We may suppose that a similar-in-type design can be applied to transformable envelopes, both roofs and facades, provided that particular joints and gaps are designed in order to allow the required movements. This short discussion is certainly not exhaustive, yet it shows how the practical implementation of the system can rely on existing knowledge and technology.

The work is not concluded. The present analysis applies to orthogonally stressed membrane or cable nets, but could be extended to more general patterns, and in particular to configurations with rotational symmetry. Of course, their arrangement strongly affects the final shape (Tibert and Pellegrino 2002; Wang et al. 2014). Another limitation consists in the proposed model, which takes into account nets that are plane in the undistorted reference configuration, undergoing small strains and large rotations, and that should certainly be complicated to account for more general finite deformations. Moreover, the soap-film analogy could be further extended to evaluate the response of the cable net under changeable boundary conditions, and specifically under a transformation of the supporting frame. In any case, the case-studies that we have just presented indicate the potentiality of this approach, demonstrating the vitality of analogic design methods to support contemporary architecture.

Acknowledgments Partial support of the European Community under Contract RFSR-CT-2012-00026 (S+G RFS-PR-11017) is gratefully acknowledged.

References

Adriaenssens S, Block P, Veenendaal D, Williams C (eds) (2014) Shell structures for architecture. form finding and optimization. Routledge, London

Aish R (1992) Computer-aided design software to augment the creation of form. In: Penz F (ed) Computer in architecture. Longman, London

Barsotti R, Ligarò SS, Royer-Carfagni G (2001) The web bridge. Int J Solids Struct 38(48–49):8831–8850

Beatini V (2015a) Polar method to design foldable plate structures. J IASS 56(2):184, 125–136

Beatini V (2015b) Translational method for designing folded plate structures. Int J Space Struct 30(2):85–97

Beatini V, Korkmaz K (2013) A transformable tensile structure. In: Bogner-Balz H, Mollaert M, Pusat E (eds) Re-Thinking lightweight structures, Tensinet. Tensinet, Istanbul

Beatini V, Royer-Carfagni G (2016) Large transformations of tensile membrane structures with moderate strains. Math Mech Solids, published on line. doi: 10.1177/1081286516643360, in press

Beghini A, Beghini LL, Schultz J, Baker WF (2013) Rankine's theorem for the design of cable structures. Struct Multidiscip Optimiz 48(5)

Bletzinger KU, Ramm E (1999) A general finite element approach to the form finding of tensile structures by the updated reference strategy. Int J Space Struct 14(2):131–145

Buchholdt HA (1999) An introduction to cable roof structures. Thomas Telford, London

Cai K (2011) A simple approach to find optimal topology of a continuum with tension-only or compression-only material. Struct Multidiscip Optim 43(6):827–835

Chen Y, You Z (2005) Mobile assemblies based on the Bennett linkage. Proc Royal Soc, Part A 461(2056):1229–1245

Feng R, Zhang LL, Wu Y, Shen S (2009) Dynamic performance of cable net facades. J Constr Steel Res 65(12):2217–2227

Fisco NR, Adeli H (2011) Smart structures. part I—active and semi-active control. Sci Iranica 26(1):275–284

Frazer JH (1995) An evolutionary architecture. Architectural association publications, London

Gantes C (2001) Deployable structures. analysis and design. WIT Press, Southampton

Guidon R (1990) Designing the design process. exploiting opportunistic thoughts. Hum Comput Interact 5:305–344

Hedgepeth JM (1982) Accuracy potentials for large space antenna reflectors with passive structure. J Spacecraft Rockets 19(3):211–217

Hilson B (1993) Basic structural behavior. understanding structures from models. Thomas Telford Ltd, London

Krish S (2011) A practical generative design method. Comput Aided Des 43(1):88–100

Lai CY, Pellegrino S (2001) Umbrella-type furlable reflector based on tension-truss concept. 42nd AIAA/ASME/ASCE/AHS/ASC structures, structural dynamics, and materials conf. and exhibit. American Institute of Aeronautics and Astronautics, Reston

Larena AB (2009) Shape design methods based on the optimisation of the structure. historical background and application to contemporary architecture. In: Kurrer KE, Lorenz W, Wetzk V (eds) Proceedings of the third international congress on construction history, Cottbus, May 2009. Neunplus1, Berlin

Logan B, Smithers T (1993) Creativity and design as exploration. In: Gero JS, Maher ML (eds) Modelling creativity and knowledge-based creative design. Erlbaum Associates, Lawrence, pp 139–175

Lynn G (1993) Folding in architecture. architectural design profile 102. Wiley, London

Menges A (2012) Material computation. higher integration in morphogenetic design. Wiley, London

Nerdinger W (2005) Frei Otto. complete works. Birkhäuser Architecture, Berlin

Preumont A (2011) Vibration control of active structures. an introduction. solid mechanics and its applications. Springer, Berlin

Rippmann M, Lachauer L, Block P (2012) Interactive vault design. Int J Space Struct 27(4):219–230

Royer-Carfagni G (1999) Wrinkled membranes and cable-stayed bridges. ASCE J Bridge Eng 4:56–62

Royer-Carfagni G (2003) Parametric-resonance-induced cable vibrations in network cable-stayed bridges. A continuum approach. J Sound Vibr 262(15):1191–1222

Salvadori MG, Tempe M (1983) Architecture and engineering. an illustrated teacher's manual on why buildings stand up. Academy of Sciences, New York

Schittich et al (2013) Detail engineering 1. Schlaich Bergermann Und Partner. Birkhauser Verlag, Berlin

Schlaich J, Moschner T (2005) Prestressed cable-net facades. Struct Eng Int 15(1):36

Shea K, Aish R, Gourtovaia M (2005) Towards integrated performance-driven generative design tools. Autom Constr 14(2):253–264

Sheck HJ (1974) The force density method for form-finding and computation of general networks. Comput Methods Appl Mech Eng 3:115–134

Szalapaj P (2001) CAD principles for architectural design. Architectural press, Oxford

Tachi T (2010) Freeform rigid-foldable structure using bidirectionally flat-foldable planar quadrilateral mesh. In: Ceccato C et al (eds) Advances in architectural geometry. Springer, Vienna, pp 87–102

Tanaka H, Natori MC (2004) Shape control of space antennas consisting of cable networks. Acta Astronaut 55(3–9):519–527

Tibert AG, Pellegrino S (2002) Deployable tensegrity reflectors for small satellites. J Spacecraft Rockets 39(5):701–709

Wang Z, Li T, Cao Y (2013) Active shape adjustment of cable net structures with pzt actuators. Aerosp Sci Technol 26(1):160–168

Wang Z, Li T, Ma X (2014) Method for generating statically determinate cable net topology configurations of deployable mesh antennas. J Struct Eng 141(7):04014182